

# Optimizing pulmonary carcinoma detection through image segmentation using evolutionary algorithms

Moulieswaran Elavarasu, Kalpana Govindaraju

Department of Computer Science, Faculty of Science and Humanities, SRM Institute of Science and Technology, Kattankulathur, India

## Article Info

### Article history:

Received Aug 19, 2023

Revised Oct 8, 2023

Accepted Dec 14, 2023

### Keywords:

Evolutionary algorithms

Image filtering

Image segmentation

Preprocessing

Pulmonary carcinoma

## ABSTRACT

This paper's goal is to suggest an image segmentation technique for use with medical images, specifically computer tomography scan images, to aid doctors in understanding the images. To address a variety of picture segmentation issues, it is necessary to investigate and apply novel evolutionary algorithms. The study focuses on pulmonary carcinoma, which is the cancer that affects males the most frequently across the globe. For proper treatment and life-saving measures, early identification of lung cancer is essential. To identify lung cancer, doctors frequently employ the computed tomography imaging technique. In order to extract tumours from lung scans, the study analyses the effectiveness of three optimization algorithms: k-means clustering, particle swarm optimization, and modified guaranteed convergence particle swarm optimization. The study also examines the pre-processing performance of four filters, namely the mean, bilateral, gaussian, and laplacian filters, shows that the bilateral filter is best suited for CT scans of the body. To test the proposed technique on 30 examples of lung scans. The proposed algorithm is tested on 30 sample lung images. The results show that the modified guaranteed convergence particle swarm optimization algorithm has the highest accuracy of 96.01%.

*This is an open access article under the CC BY-SA license.*



## Corresponding Author:

Kalpana Govindaraju

Department of Computer Science, Faculty of Science and Humanities, SRM Institute of Science and Technology  
Kattankulathur, Chennai-603203, India

Email: kalpanag@srmist.edu.in

## 1. INTRODUCTION

Pulmonary carcinoma is one of the most common and deadliest types of cancer worldwide. Early detection is crucial for successful treatment and improved patient outcomes. Medical imaging techniques, such as computed tomography (CT) scans, are widely used for the diagnosis and monitoring of pulmonary carcinoma. However, accurately detecting cancerous regions from medical images can be challenging due to the complexity of lung structures and variations in image quality. In recent years, machine-learning techniques, such as support vector machines (SVM), have been increasingly used in biomedical image processing for the detection of pulmonary carcinoma. SVMs are a type of supervised learning algorithm that has been widely used in various fields, including image processing, natural language processing, and computer vision. SVMs are particularly useful in solving classification problems, which makes them suitable for detecting cancerous regions from medical images [1]. The use of evolutionary algorithms in automated systems for pulmonary carcinoma detection several benefits, including increased accuracy, reduced inter-observer variability, and improved efficiency. These systems can also provide early detection of pulmonary carcinoma, which can significantly improve patient outcomes [1]. The choice of noise removal and filtering technique depends on the type and level of noise present in the image and the specific application of the image. Moreover, the effectiveness of these techniques also depends on the quality of the

image, the imaging modality used, and the parameters selected for the filter. In this paper, we propose an automated system for pulmonary carcinoma detection using image segmentation by means of various evolutionary algorithms. We compare the performance of different evolutionary algorithms, including genetic algorithms, particle swarm optimization (PSO), differential evolution, and artificial bee colony optimization, for pulmonary carcinoma detection. We also evaluate the performance of different segmentation techniques, including thresholding, region-based segmentation, and edge-based segmentation, with different evolutionary algorithms. The proposed system is evaluated using a dataset of CT images, and the results are compared with the ground truth. The potential of evolutionary algorithms in improving the accuracy and efficiency of pulmonary carcinoma detection is emphasized, along with areas for further research and development [2].

## 2. RELATED WORK

K-means clustering is a technique used for analyzing CT images and localizing lung tumors. It involves several steps such as preprocessing the images, extracting the region of interest (ROI), extracting meaningful features, creating a feature matrix, determining the number of clusters, applying k-means clustering, and localizing the tumors based on the centroids of the clusters. However, it is important to note that the accuracy of this approach depends on various factors and combining multiple techniques may be necessary for results that are more reliable [3].

The combination of k-means clustering and Cuckoo Search optimization is proposed as an effective method for improving lung cancer segmentation in CT scans. K-means clustering is used to separate tumor regions from healthy lung tissue, while Cuckoo Search optimizes the clustering solution to enhance segmentation accuracy. The algorithm iteratively updates the positions of candidate solutions based on their fitness, aiming to find the optimal clustering configuration. This combined approach leverages the strengths of both methods and can be followed by post-processing techniques for further refinement. However, the performance of the method may vary depending on implementation, parameters, and dataset characteristics, necessitating proper validation and evaluation [4].

Foggy k-means, also known as fuzzy k-means, is a clustering algorithm used to cluster data points with uncertain or ambiguous membership. When applying foggy k-means to lung cancer data, the general steps involve data preprocessing, initializing cluster centroids, calculating membership degrees for each data point, updating cluster centroids based on the membership degrees, repeating these steps until convergence, assigning data points to clusters based on their highest membership degree, and interpreting and evaluating the resulting clusters. The algorithm allows for data points to belong to multiple clusters with varying degrees of membership. It is important to adapt the algorithm to the specific dataset and use appropriate evaluation measures [5].

In the optimal reactive power dispatch (ORPD) problem, PSO is a commonly used algorithm. To enhance its performance, a modified inertia weight control strategy can be employed. The strategy involves adjusting the inertia weight during the optimization process to balance exploration and exploitation effectively. The steps include initialization, fitness evaluation, global best update, particle movement, inertia weight update, and termination. The modified strategy can be linearly decreasing or nonlinear, depending on the desired decay rate. By using this approach, PSO can find near-optimal solutions for the ORPD problem. Experimentation and parameter tuning may be necessary for optimal performance [6].

Convergence-guaranteed PSO methods for mobile robot global path planning aim to improve the convergence properties of PSO by incorporating various techniques. These techniques include designing an appropriate fitness function, handling constraints, using adaptive parameters, incorporating local search strategies, preserving diversity within the swarm, and hybridizing with other algorithms. By combining these techniques, convergence-guaranteed PSO methods enhance the optimization process, enabling the generation of optimal paths while considering obstacles and constraints. It is important to experiment and select the most effective approach based on the specific path planning problem [7].

The improved convergence particle swarm optimization (CPSO) algorithm with random sampling of control parameters enhances the traditional CPSO algorithm by incorporating random sampling. This allows for better exploration of the search space, improving the chances of finding optimal solutions and avoiding local optima. The algorithm initializes a swarm of particles, updates their velocities and positions based on control parameters, evaluates fitness, and performs random sampling of control parameters. It continues this process until a termination criterion is met. The algorithm aims to converge faster and produce better solutions compared to standard CPSO. However, experimentation and fine-tuning may be required for optimal performance depending on the problem at hand [8].

In summary, to use PSO for generating stable structures of carbon clusters ( $C_n$ , where  $n=3-6, 10$ ), you would initialize a population of particles representing carbon cluster structures. Each particle's position represents the coordinates of carbon atoms within the cluster. The velocity and position of each particle are

updated based on its current position, best personal position, and best global position found by the swarm. The potential energy or stability of each structure is evaluated using an objective function. Constraints can be applied to ensure structural integrity. The algorithm iteratively searches for structures with low potential energy, updating personal and global best positions along the way. The process continues until a termination criterion is met, such as reaching a maximum number of iterations or achieving a desired level of stability [9].

### 3. METHOD

Accuracy is critical in medical image segmentation since it involves human lives. It is critical to eliminate noise content and improve image quality before an evaluation [10]. The operational approach for the current study is shown in Figure 1. The medical images from the Kaggle dataset which contains scans of 1,098 unique individuals, selected as the source for input CT images, these are grouped into 3 clusters consist of 120 Benign cases, 562 Malignant cases, and 416 Normal cases.

Since it involves human lives, precision is of utmost importance in medical picture segmentation. Prior to an inspection, it is imperative to reduce the occurrence of noise content and to enhance image quality. Preprocessing is the term for this stage of the work. Noise removal and contrast enhancement are the two main procedures in the preprocessing stage. The effectiveness of mean, bilateral, gaussian, and laplacian filters to isolate the existence of speckle noise has been compared in the current work. Segmentation is the second phase of the work. Applying three techniques-k-means, PSO and modified guaranteed convergence particle swarm optimization (MGCP SO)-is what this stage entails. The segmentation results of the five procedures mentioned above were split up, and the tumour component was retrieved and manually excised. The outcomes demonstrate that the segmentation based on the MGCP SO is more accurate than the others.

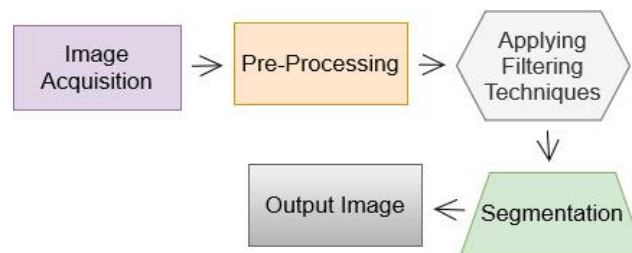


Figure 1. Process flow diagram

#### 3.1. Image acquisition

The process of collecting a picture from a source, often hardware equipment such as cameras, is referred to as image acquisition. Images from intrinsically electronic devices such as CT and magnetic resonance imaging (MRI) should be acquired via direct digital DICOM capture. Digital interfaces gather and transport high-resolution image data from modality and grayscale. Meanwhile, analogue frame grabbers convert the voltage output of a video signal, such as a scanning console display, into an image. The frame-grabbing method, like printing an image to film, limits image quality to only 8 bits, whereas colour data is collected at 12, 16, or even 32 bits. Capturing in 8 bits may limit the image's ability to display all clinical data, levels, contrast, and brightness settings. The initial stage in image processing techniques is to read input images from a designated source for later processing. By smoothing the image, Gaussian noise and spatial filtering are removed [11].

#### 3.2. Pre-processing

Preprocessing the grayscale image to reduce noise is the first step. The gaussian filter, bilateral filter, laplacian filter, and mean filter are a few examples of filtering methods. Table 1 represents the various filtering techniques, description, advantages and its disadvantages [12]–[22].

#### 3.3. K-Means clustering algorithm

The k-means clustering algorithm is the most basic and widely used method in cluster analysis. This programme divides a dataset into two or more clusters. The accuracy of this procedure is entirely dependent on the cluster centre chosen. To achieve the best results, the best cluster centre must be chosen. The general measure used to separate the dataset is the Euclidean distance. The Euclidean distance is used to allocate pixels to separate clusters. In this algorithm, the objective function is:

$$J(v) = \sum_{i=1}^C \sum_{j=1}^{C_i} (\|x_i - v_j\|)^2 \quad (1)$$

where  $x_i$  represent pixels,  $v_j$  represent cluster centres,  $\|x_i - v_j\|$  is the Euclidean distance between  $x_i$  and  $v_j$ ,  $C_i$  represents the number of data points for the  $i$ th cluster, and  $C$  represents the number of cluster centres [23], [24].

Table 1. Various filtering techniques [12]–[22]

Algorithm	Description	Advantages	Disadvantages
Gaussian	Image blurring to minimise noise	Removes Gaussian noise effectively and retains edges better than the mean filter.	edges are blurred, which might not be ideal for photos containing non-Gaussian noise.
Bilateral	Based on spatial and range information, it smooths the image while keeping the edges.	Removes noise while keeping edges, with less smoothing than the Gaussian filter.	Slower than other filters and maybe ineffective for photographs with intricate textures.
Laplacian	Edge enhancement is achieved by subtracting the blurred picture from the original image.	Edges are preserved, thus edge detection jobs are possible.	Amplifies noise, may not be effective for low contrast images.
Mean	Replaces each pixel with the mean value of its neighbours.	Effectively reduces noise and better maintains edges than the Gaussian filter	Edges are blurred, therefore they might not be ideal for high-frequency noisy photos.

### 3.4. Particle swarm optimization

PSO is a metaheuristic algorithm used extensively in medical image analysis. It mimics the social behaviours of birds seeking food. The primary idea behind PSO is information sharing and communication. In this method, each particle has an initial position and velocity. The fitness value is used to update the velocity and position. The relevant PSO equations for updating location and velocity are [25]:

$$v(t+1) = v(t) + c_1 r_1 [pbest(t) - x(t)] + c_2 r_2 [gbest(t) - x(t)], x(t+1) = x(t) + v(t+1) \quad (2)$$

where  $r_1$  and  $r_2$  are the random integers and  $c_1$  and  $c_2$  are the acceleration coefficients. PSO's success is dependent on the fitness function. The following fitness function was utilised in this study:

$$\text{maximize } f = \sum_{i=1}^n \frac{\text{intercluster distance}}{\text{intracluster distance}} \quad (3)$$

### 3.5. Modified guaranteed convergence particle swarm optimization

The MGCPSO focuses on a new particle that deals with the region's current best location. This particle is handled as a member of the swarm in this task, and the velocity update equation for this new particle is as follows [26]:

$$v\varphi(t+1) = x\varphi(t) + pbest(t) + \omega v\varphi(t) + \rho(t) (1 - 2r) \quad (4)$$

The social component improves the search ability. This will improve the random search in the area of the gbest position.

## 4. RESULT AND DISCUSSION

The techniques are being practically applied in Python code with the aid of Jupyter and Google Colab, and the outcomes are being validated. Several filters, including mean, bilateral, gaussian, and laplacian filters, were compared in the initial step of preprocessing. Table 2 displays the streptomyces subtilisin inhibitor (SSI) and streptomyces metallo-protease inhibitor (SMPI) values. The results show that the bilateral filter is more accurate than the mean, bilateral, gaussian, and laplacian filters for segmenting medical images. By contrasting the algorithm's outputs with manual segmentation results, the true positive rate, true negative rate, false positive rate, and false negative rate were used to gauge the accuracy of the segmentation. Figure 2 display the preprocessed results of the images. In Table 3, numerical outcomes for k-means algorithm are displayed, Table 4 displays the numerical outcomes for PSO algorithm. Table 5 displays the numerical outcomes for MGCPSO algorithm, Table 6 displays the statistical comparative result of accuracy, and Table 7 represents the comparative evaluation of the predicted method's accuracy.

Table 2. SMPI and SSI values of input images

Sample Images	SMPI				SSI			
	Mean	Bilateral	Gaussian	Laplacian	Mean	Bilateral	Gaussian	Laplacian
Image 1	1.00005099	0.99883772	1.00015143	0.99983883	0.00653812	0.00207065	0.00548567	0.685815
Image 2	1.00006564	0.99885763	1.00016626	0.99982655	0.00656545	0.00202673	0.00550924	0.685577
Image 3	1.00006497	0.99880494	1.00013502	0.99980607	0.00649593	0.00200639	0.0054503	0.68777
Image 4	1.00007082	0.99880084	1.00014042	0.99979297	0.0065783	0.0020208	0.00552204	0.686029
Image 5	1.00008755	0.99886379	1.00013866	0.99975728	0.00584951	0.00150239	0.00490082	0.70714
Image 6	1.00008619	0.9887512	1.00014111	0.99975457	0.00572866	0.00151213	0.00480674	0.708324
Image 7	1.00002471	0.99949843	0.99985296	0.99997888	0.00574208	0.00169107	0.00480342	0.719542
Image 8	0.99998011	0.99876035	0.99985778	0.99996715	0.00588469	0.00173544	0.00492531	0.714687
Image 9	1.0000285	0.99876677	0.99989671	0.99996982	0.00600199	0.00172164	0.00503817	0.710399
Image 10	1.00001908	0.99928420	1.00000917	0.99996443	0.00616713	0.00172735	0.0051611	0.702873
Image 11	1.00001004	0.99933914	0.99996487	0.99996091	0.00611228	0.00161426	0.00513139	0.702475
Image 12	1.00001499	0.99940113	1.00003242	0.99995779	0.00587849	0.00164259	0.00493284	0.706968
Image 13	1.00001268	0.99927493	1.00002306	0.99995558	0.00277204	0.00127928	0.00233801	0.776927
Image 14	1.00001508	0.99908803	1.00001072	0.99995312	0.00363379	0.00174865	0.00306998	0.739167
Image 15	1.00002226	0.99909637	1.00003674	0.99995350	0.00378776	0.00169811	0.00319446	0.734687
Image 16	1.00001885	0.99912012	1.00006004	0.99993713	0.00367232	0.00104465	0.00309586	0.728587
Image 17	1.00001577	0.99911254	1.00003237	0.99996591	0.00374972	0.00102567	0.00315888	0.727015
Image 18	1.00001296	0.99928709	1.00007336	0.99996315	0.00378583	0.00112909	0.0031973	0.723038
Image 19	1.00002629	0.99931720	1.00004326	0.99996596	0.00372441	0.00137282	0.00314496	0.72536
Image 20	0.99998131	0.99972701	0.99981695	0.99996780	0.00407759	0.00127076	0.00342971	0.714843
Image 21	1.00001090	0.99846019	0.99996623	0.99997494	0.00394663	0.00128628	0.00333205	0.717366
Image 22	1.00001165	0.99846254	1.00002183	0.99997072	0.00397981	0.00134342	0.00335919	0.716257
Image 23	1.00002200	0.99843795	1.00002915	0.99997714	0.00395729	0.00122709	0.00333939	0.721084
Image 24	1.00000463	0.99841464	1.00002746	0.99997623	0.00351772	0.00099441	0.00297505	0.731775
Image 25	1.00002220	0.99858012	1.00001403	0.99997446	0.00353507	0.00103015	0.00298315	0.736536
Image 26	1.00000053	0.99857502	1.00001434	0.99997606	0.00145602	0.00093932	0.00322325	0.828436
Image 27	1.00000855	0.99855847	1.00000520	0.99997855	0.00606584	0.00158877	0.00510341	0.677864
Image 28	1.00000874	0.99854366	0.99997554	0.99998330	0.00639493	0.00177743	0.00538764	0.669129
Image 29	1.00009861	0.99886061	1.00013501	0.99973294	0.00646719	0.00183678	0.00545048	0.665425
Image 30	1.00008776	0.99886256	1.00018278	0.99973633	0.0065535	0.00185939	0.00552473	0.662408

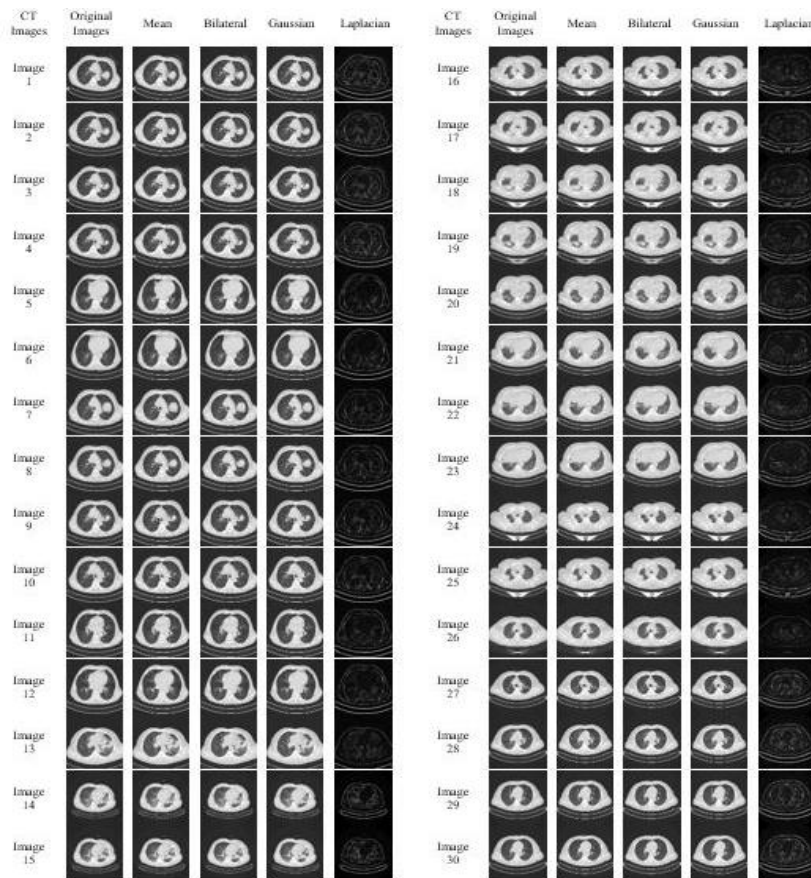


Figure 2. After preprocessing

Table 3. Numerical outcomes for k-means algorithm

Images	True positive rate	True negative rate	False positive rate	False negative rate	Accuracy
Image 1	83.0198	88.4375	16.9802	11.5625	85.7287
Image 2	86.0726	81.3622	13.9274	18.6378	83.7174
Image 3	78.4182	89.1677	21.5818	10.8323	83.793
Image 4	85.3457	82.7848	14.6543	17.2152	84.0653
Image 5	78.4954	78.8414	21.5046	21.1586	78.6684
Image 6	85.7631	85.6644	14.2369	14.3356	85.7138
Image 7	87.8826	77.4612	12.1174	22.5388	82.6719
Image 8	85.4438	89.7083	14.5562	10.2917	87.5761
Image 9	83.6784	83.5609	16.3216	16.4391	83.6197
Image 10	76.5976	80.3489	23.4024	19.6511	78.4733
Image 11	79.4071	80.2404	20.5929	19.7596	79.8238
Image 12	77.1947	87.7569	22.8053	12.2431	82.4758
Image 13	81.3153	79.0573	18.6847	20.9427	80.1863
Image 14	82.2217	77.6233	17.7783	22.3767	79.9225
Image 15	87.8811	87.4071	12.1189	12.5929	87.6441
Image 16	76.4974	89.9263	23.5026	10.0737	83.2119
Image 17	82.4508	77.1854	17.5492	22.8146	79.8181
Image 18	86.9717	88.1683	13.0283	11.8317	87.57
Image 19	80.0838	89.8913	19.9162	10.1087	84.9876
Image 20	79.6117	89.3348	20.3883	10.6652	84.4733
Image 21	82.2061	85.9213	17.7939	14.0787	84.0637
Image 22	84.5572	87.1664	15.4428	12.8336	85.8618
Image 23	79.2736	81.4655	20.7264	18.5345	80.3696
Image 24	79.0333	89.4537	20.9667	10.5463	84.2435
Image 25	82.7447	88.289	17.2553	11.711	85.5169
Image 26	87.3402	87.9803	12.6598	12.0197	87.6603
Image 27	78.4169	88.049	21.5831	11.951	83.233
Image 28	81.1904	85.3374	18.8096	14.6626	83.2639
Image 29	83.385	83.557	16.615	16.443	83.471
Image 30	81.926	86.5422	18.074	13.4578	84.2341

Table 4. Numerical outcomes for PSO algorithm

Images	True positive rate	True negative rate	False positive rate	False negative rate	Accuracy
Image 1	78.3473	83.7745	21.6527	17.4683	81.0609
Image 2	87.7165	82.5317	12.2835	11.8226	85.1241
Image 3	85.0788	88.1774	14.9212	12.504	86.6281
Image 4	80.7158	87.496	19.2842	18.8781	84.1059
Image 5	77.2816	81.1219	22.7184	15.186	79.20175
Image 6	85.578	84.814	14.422	15.1669	85.196
Image 7	77.5807	84.8331	22.4193	17.5781	81.2069
Image 8	81.6709	82.4219	18.3291	14.9456	82.0464
Image 9	79.424	85.0544	20.576	12.0061	82.2392
Image 10	81.1218	87.9939	18.8782	17.1153	84.55785
Image 11	83.3637	82.8847	16.6363	12.8556	83.1242
Image 12	83.5755	87.1444	16.4245	10.3926	85.35995
Image 13	88.0024	89.6074	11.9976	12.4266	88.8049
Image 14	88.1423	87.5734	11.8577	16.7596	87.85785
Image 15	77.2572	83.2404	22.7428	18.2952	80.2488
Image 16	88.4797	81.7048	11.5203	13.7834	85.09225
Image 17	83.8806	86.2166	16.1194	19.5936	85.0486
Image 18	80.8995	80.4064	19.1005	16.3412	80.65295
Image 19	81.5196	83.6588	18.4804	18.2952	82.5892
Image 20	78.789	86.0371	21.211	13.9629	82.41305
Image 21	86.727	80.0248	13.273	19.9752	83.3759
Image 22	84.945	81.7717	15.055	18.2283	83.35835
Image 23	87.1483	82.4668	12.8517	17.5332	84.80755
Image 24	79.8254	80.315	20.1746	19.685	80.0702
Image 25	81.0092	83.7164	18.9908	16.2836	82.3628
Image 26	77.3288	87.0294	22.6712	12.9706	82.1791
Image 27	79.8118	84.8031	20.1882	15.1969	82.30745
Image 28	81.0954	89.095	18.9046	10.905	85.0952
Image 29	84.5016	79.0836	15.4984	20.9164	81.7926
Image 30	85.4518	80.8443	14.5482	19.1557	83.14805

Lung cancer detection has been done in prior studies, 89.5% accuracy was achieved utilising PSO, genetic optimisation, the SVM algorithm, and the Gabor filter [27]. A maximum accuracy of 90% was achieved utilising the genetic algorithm and k-nearest neighbor (K-NN) classification to identify lung cancer [28]. Figure 3 displays the relative outcomes of the true positive rate value, Figure 4 displays the relative outcomes of

the true negative rate value, Figure 5 displays the relative outcomes of the false positive rate value, Figure 6 displays the relative outcomes of the false negative rate value. Figure 7 represents the outcomes of accuracy, Figure 8 display the accuracy.

Table 5. Numerical outcomes for MGCP SO algorithm

Images	True positive rate	True negative rate	False positive rate	False negative rate	Accuracy
Image 1	85.5901	97.894	14.4099	2.106	91.74205
Image 2	92.1561	97.4464	7.8439	2.5536	94.80125
Image 3	85.9277	95.4679	14.0723	4.5321	90.6978
Image 4	88.0733	97.7006	11.9267	2.2994	92.88695
Image 5	88.036	98.8191	11.964	1.1809	93.42755
Image 6	88.9129	97.8826	11.0871	2.1174	93.39775
Image 7	89.5582	97.1109	10.4418	2.8891	93.33455
Image 8	87.7662	95.9419	12.2338	4.0581	91.85405
Image 9	90.925	97.5847	9.075	2.4153	94.25485
Image 10	94.3613	97.6492	5.6387	2.3508	96.00525
Image 11	91.4426	98.4483	8.5574	1.5517	94.94545
Image 12	88.2684	97.1438	11.7316	2.8562	92.7061
Image 13	92.4882	98.5891	7.5118	1.4109	95.53865
Image 14	85.1011	98.428	14.8989	1.572	91.76455
Image 15	88.4775	98.4377	11.5225	1.5623	93.4576
Image 16	85.8022	95.6501	14.1978	4.3499	90.72615
Image 17	85.6168	98.8983	14.3832	1.1017	92.25755
Image 18	84.5809	95.9124	15.4191	4.0876	90.24665
Image 19	84.935	96.9602	15.065	3.0398	90.9476
Image 20	91.0548	98.9336	8.9452	1.0664	94.9942
Image 21	84.6432	95.7747	15.3568	4.2253	90.20895
Image 22	87.7662	96.7971	12.2338	3.2029	92.28165
Image 23	87.7271	98.4374	12.2729	1.5626	93.08225
Image 24	85.9182	96.7405	14.0818	3.2595	91.32935
Image 25	85.2057	95.9214	14.7943	4.0786	90.56355
Image 26	90.1859	97.8667	9.8141	2.1333	94.0263
Image 27	87.2679	97.837	12.7321	2.163	92.55245
Image 28	84.3414	96.8343	15.6586	3.1657	90.58785
Image 29	89.5071	96.0861	10.4929	3.9139	92.7966
Image 30	90.8882	95.9334	9.1118	4.0666	93.4108

Table 6. Statistical comparative result of accuracy

Images	K-means	PSO	MGCP SO
Image 1	85.7287	81.0609	91.74205
Image 2	83.7174	85.1241	94.80125
Image 3	83.793	86.6281	90.6978
Image 4	84.0653	84.1059	92.88695
Image 5	78.6684	79.20175	93.42755
Image 6	85.7138	85.196	93.39775
Image 7	82.6719	81.2069	93.33455
Image 8	87.5761	82.0464	91.85405
Image 9	83.6197	82.2392	94.25485
Image 10	78.4733	84.55785	96.00525
Image 11	79.8238	83.1242	94.94545
Image 12	82.4758	85.35995	92.7061
Image 13	80.1863	88.8049	95.53865
Image 14	79.9225	87.85785	91.76455
Image 15	87.6441	80.2488	93.4576
Image 16	83.2119	85.09225	90.72615
Image 17	79.8181	85.0486	92.25755
Image 18	87.57	80.65295	90.24665
Image 19	84.9876	82.5892	90.9476
Image 20	84.4733	82.41305	94.9942
Image 21	84.0637	83.3759	90.20895
Image 22	85.8618	83.35835	92.28165
Image 23	80.3696	84.80755	93.08225
Image 24	84.2435	80.0702	91.32935
Image 25	85.5169	82.3628	90.56355
Image 26	87.6603	82.1791	94.0263
Image 27	83.233	82.30745	92.55245
Image 28	83.2639	85.0952	90.58785
Image 29	83.471	81.7926	92.7966
Image 30	84.2341	83.14805	93.4108

Table 7. Comparative evaluation of the predicted method's accuracy

Numerous techniques	Accuracy
PSO, Genetic Algorithm, and SVM algorithm [27]	89.5%
K-NN classification using genetic algorithm [28]	90%
MGCP SO	96.01%

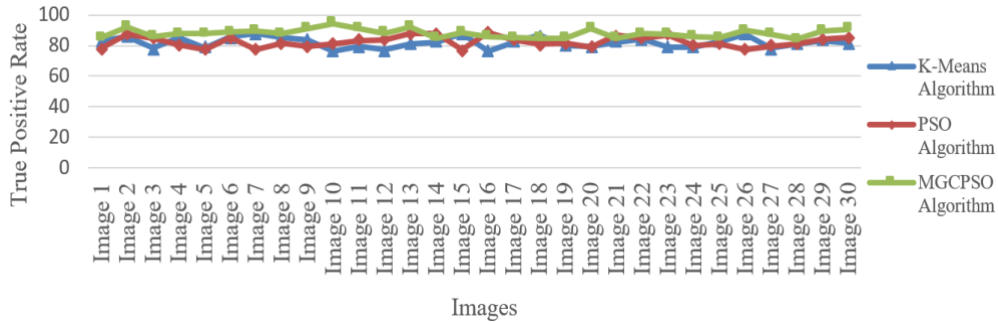


Figure 3. Relative outcomes of the true positive rate value

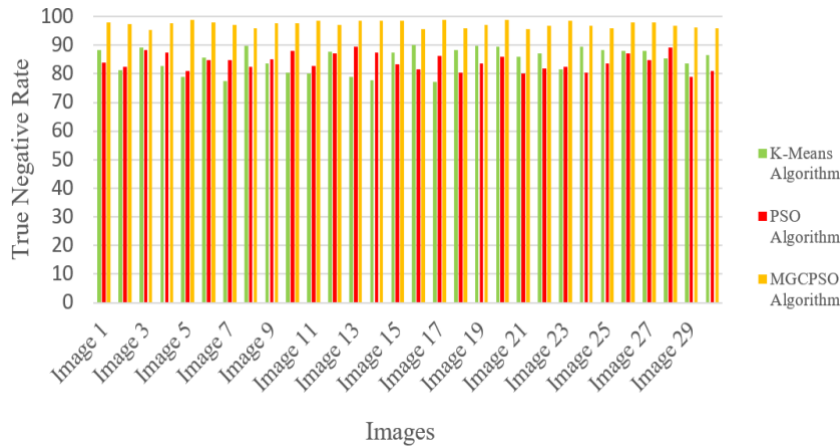


Figure 4. Relative outcomes of the true negative rate value

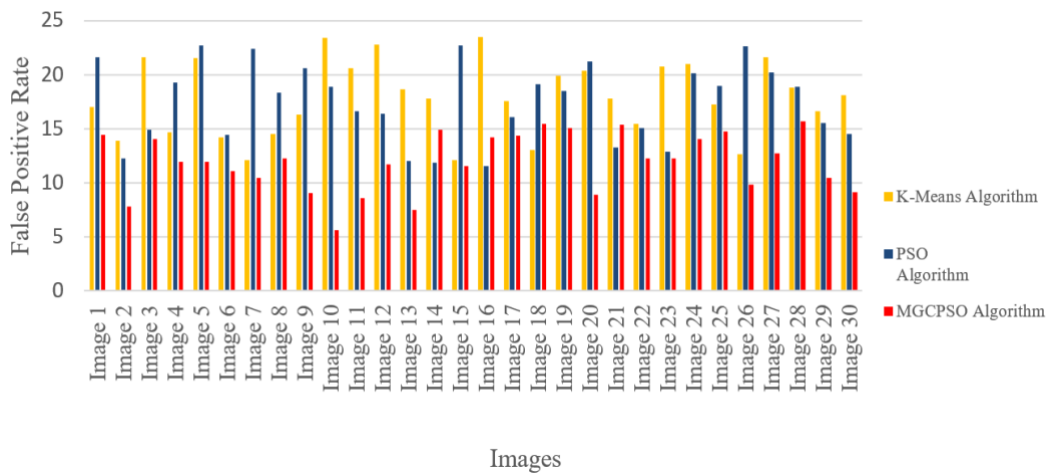


Figure 5. Relative outcomes of the false positive rate value



Figure 6. Relative outcomes of the false negative rate value

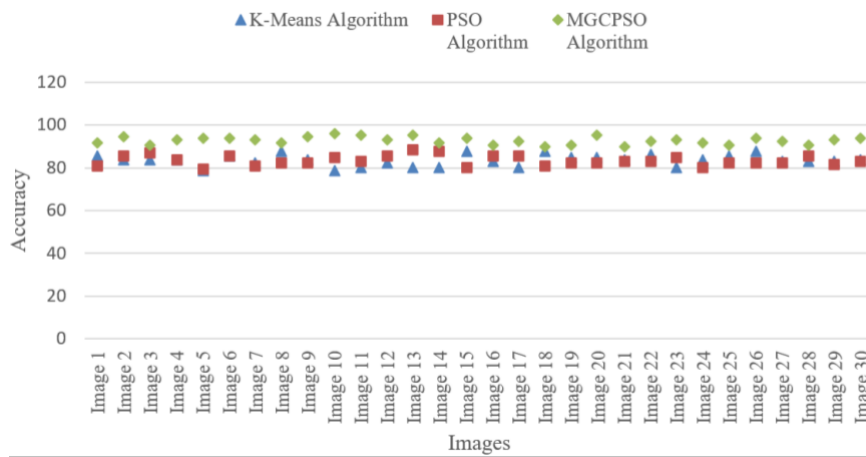


Figure 7. Outcomes of accuracy

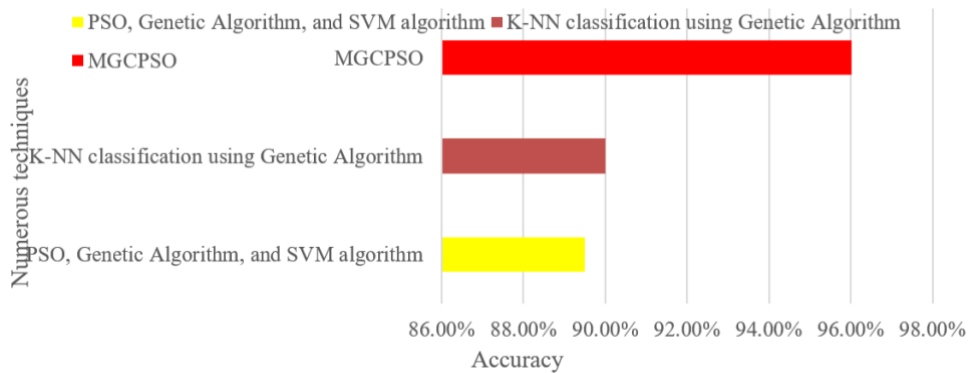


Figure 8. Accuracy

### 5. CONCLUSION

Optimizing pulmonary carcinoma detection through image segmentation using evolutionary algorithms is a promising approach to improve the accuracy of diagnosis from medical images. By leveraging the power of evolutionary algorithms, the segmentation parameters of the image segmentation algorithm can be optimized to achieve better results. The process involves several key steps, including dataset preparation, preprocessing, image segmentation, fitness function design, evolutionary algorithm design, chromosome

encoding, initialization, fitness evaluation, selection, variation operators, fitness update, replacement, termination criteria, and evaluation. These steps work together iteratively to refine the image segmentation algorithm and enhance its ability to detect and differentiate pulmonary carcinoma regions from healthy lung tissue. The use of evolutionary algorithms allows for the exploration of a vast parameter space, gradually converging towards better solutions. By evaluating the fitness of each chromosome based on the accuracy of the segmentation results, the algorithm can guide the optimization process towards more accurate and reliable segmentation. It is important to note that the success of this approach relies on various factors, such as the quality and representativeness of the training dataset, the design of the fitness function, and the selection of appropriate evolutionary algorithm parameters. Additionally, the optimized image segmentation algorithm should be evaluated on separate validation or testing images to ensure its generalizability and effectiveness. Overall, by leveraging evolutionary algorithms to optimize the image segmentation process, the accuracy and efficiency of pulmonary carcinoma detection can be significantly improved, thereby aiding in early diagnosis and improving patient outcomes. This approach holds great potential for advancing the field of medical imaging and facilitating more precise and timely detection of pulmonary carcinoma.

## REFERENCES

- [1] M. Kurkure and A. Thakare, "Introducing automated system for lung cancer detection using evolutionary approach," *International Journal of Engineering and Computer Science*, vol. 5, no. 5, pp. 16736-16739, 2016, doi: 10.18535/ijecs/v5i5.69.
- [2] N. Kumar and M. Nachamai, "Noise removal and filtering techniques used in medical images," *Oriental Journal of Computer Science and Technology*, vol. 10, no. 1, pp. 103-113, 2017, doi: 10.13005/ojcs/10.01.14.
- [3] A. C. G. and R. M. S., "Analysis of CT images and localization of lung tumor using k-means clustering," *Advances in Computational Sciences and Technology*, vol. 12, no. 1, pp. 45-51, 2019.
- [4] P. Singh, P. Nanglia, and D. A. N. Mahajan, "Improved lung cancer segmentation using k-means and cuckoo search," *International Journal of Innovative Technology and Exploring Engineering*, vol. 9, no. 2, pp. 3746-3757, 2019, doi: 10.35940/ijitee.b6221.129219.
- [5] A. K. Yadav, D. Tomar, and S. Agarwal, "Clustering of lung cancer data using foggy k-means," *2013 International Conference on Recent Trends in Information Technology, ICRTIT 2013*, pp. 13-18, 2013, doi: 10.1109/ICRTIT.2013.6844173.
- [6] M. Sabir, A. Ahmad, A. Ahmed, S. Siddique, and U. A. Hashmi, "A modified inertia weight control of particle swarm optimization for optimal reactive power dispatch problem," *2021 International Conference on Emerging Power Technologies, ICEPT 2021*, 2021, doi: 10.1109/ICEPT51706.2021.9435588.
- [7] B. Tang, Z. Zhanxia, and J. Luo, "A convergence-guaranteed particle swarm optimization method for mobile robot global path planning," *Assembly Automation*, vol. 37, no. 1, pp. 114-129, 2017, doi: 10.1108/AA-03-2016-024.
- [8] G. Jana, A. Mitra, S. Pan, S. Sural, and P. K. Chattaraj, "Modified particle swarm optimization algorithms for the generation of stable structures of carbon clusters, Cn (n=3-6, 10)," *Frontiers in Chemistry*, vol. 7, 2019, doi: 10.3389/fchem.2019.00485.
- [9] L. Sun, X. Song, and T. Chen, "An improved convergence particle swarm optimization algorithm with random sampling of control parameters," *Journal of Control Science and Engineering*, vol. 2019, 2019, doi: 10.1155/2019/7478498.
- [10] A. G. N. Panpaliya, N. Tadas, S. Bobade, R. Aglawe, "A survey on early detection and prediction of lung cancer," *International Journal of Computer Science and Mobile Computing*, vol. 4, no. 1, pp. 175-184, 2015.
- [11] K. J. Dreyer, J. H. Thrall, D. S. Hirschorn, and A. Mehta, "PACS: A guide to the digital revolution: second edition," *PACS: A Guide to the Digital Revolution: Second Edition*, pp. 1-579, 2006, doi: 10.1007/0-387-31070-3.
- [12] P. P. Shetti and A. P. Patil, "Performance comparison of mean, median and wiener filter in MRI image de-noising," *International Journal for Research Trends and Innovation*, vol. 2, no. 6, 2017.
- [13] J. Joseph and R. Periyasamy, "An image driven bilateral filter with adaptive range and spatial parameters for denoising magnetic resonance images," *Computers and Electrical Engineering*, vol. 69, pp. 782-795, 2018, doi: 10.1016/j.compeleceng.2018.02.033.
- [14] D. Devasena, K. Srinivasan, B. Sharmila, and A. Booja, "Despeckling algorithms for removing noise in medical images," *Turkish Journal of Computer and Mathematics Education (TURCOMAT)*, vol. 12, no. 6, pp. 87-94, 2021, doi: 10.17762/turcomat.v12i6.1271.
- [15] G. Deng and L. W. Cahill, "Adaptive Gaussian filter for noise reduction and edge detection," *IEEE Nuclear Science Symposium & Medical Imaging Conference*, no. pt 3, pp. 1615-1619, 1994, doi: 10.1109/nssmic.1993.373563.
- [16] A. Singh, "Comparative analysis of Gaussian filter with wavelet denoising for various noises present in images," *Indian Journal of Science and Technology*, vol. 9, no. 1, pp. 1-8, 2016, doi: 10.17485/ijst/2016/v9i47/106843.
- [17] T. Barbu, "Gabor filter-based face recognition technique," *Proceedings of the Romanian Academy Series A - Mathematics Physics Technical Sciences Information Sciences*, vol. 11, no. 3, pp. 277-283, 2010.
- [18] A. Kafuo, S. Diaf, A. Gonifeda, and A. Baba, "A literature survey of Gabor filter and its application," *Technical Report*, 2017, doi: 10.13140/RG.2.2.11079.50085.
- [19] S. Paris, S. W. Hasinoff, and J. Kautz, "Local Laplacian filters: edge-aware image processing with a Laplacian pyramid," *Communications of the ACM*, vol. 58, no. 3, pp. 81-91, 2015, doi: 10.1145/2723694.
- [20] M. Aubry, S. Paris, S. W. Hasinoff, J. Kautz, and F. Durand, "Fast local laplacian filters: theory and applications," *ACM Transactions on Graphics*, vol. 33, no. 5, 2014, doi: 10.1145/2629645.
- [21] Y. Zhu and C. Huang, "An improved median filtering algorithm for image noise reduction," *Physics Procedia*, vol. 25, pp. 609-616, 2012, doi: 10.1016/j.phpro.2012.03.133.
- [22] T. M. Sheeba and S. A. A. Raj, "Analysis of noise removal techniques on retinal optical coherence tomography images," *International Journal of Advanced Computer Science and Applications*, vol. 13, no. 9, pp. 422-427, 2022, doi: 10.14569/IJACSA.2022.0130948.
- [23] K. Venkatalakshmi and S. Mercy Shalinie, "Classification of multispectral images using support vector machines based on PSO and K-means clustering," *Proceedings-2005 International Conference on Intelligent Sensing and Information Processing, ICISIP'05*, vol. 2005, pp. 127-133, 2005, doi: 10.1109/ICISIP.2005.1529435.
- [24] K. Venkatalakshmi and S. M. Shalinie, "Multispectral image classification using modified k-means algorithm," *Neural Network World*, vol. 17, no. 2, pp. 113-120, 2007.

- [25] H. Gao, C. M. Pun, and S. Kwong, "An efficient image segmentation method based on a hybrid particle swarm algorithm with learning strategy," *Information Sciences*, vol. 369, pp. 500–521, 2016, doi: 10.1016/j.ins.2016.07.017.
- [26] P. K. Patel, V. Sharma, and K. Gupta, "Guaranteed convergence particle swarm optimization using personal best," *International Journal of Computer Applications*, vol. 73, no. 7, pp. 6–10, 2013, doi: 10.5120/12751-9694.
- [27] A. Asuntha, N. Singh, A. Srinivasan, and A. Professor, "PSO, genetic optimization and SVM algorithm used for lung cancer detection," Available online [www.jocpr.com](http://www.jocpr.com) *Journal of Chemical and Pharmaceutical Research*, vol. 8, no. 6, pp. 351–359, 2016.
- [28] P. Bhuvanewari and A. B. Therese, "Detection of cancer in lung with K-NN classification using genetic algorithm," *Procedia Materials Science*, vol. 10, pp. 433–440, 2015, doi: 10.1016/j.mspro.2015.06.077.

## BIOGRAPHIES OF AUTHORS



**Moulieswaran Elavarasu**     is pursuing Ph.D. in Computer Science from Faculty of Science and Humanities, SRM Institute of Science and Technology, Chennai. He completed his B.Sc. Computer Science from Periyar University, Salem, Completed his M.C.A., from Anna University, Coimbatore and completed his M.Phil. Computer Science in Periyar University, Salem. Previously he had 8.5 years of teaching experience at M.G.R. College, Hosur. His research work mainly focuses on machine learning techniques in detection of pulmonary carcinoma. He can be contacted at email: [emoulieswaran@gmail.com](mailto:emoulieswaran@gmail.com).



**Kalpana Govindaraju**     has completed her Ph.D. from SRM Institute of Science and Technology. Her Current research focuses on parallel and distributed computing, block chain technology, machine learning, and cloud security. Currently, she is working as a Professor and Head in the Department of Computer Science, Faculty of Science and Humanities, SRM Institute of Science and Technology, Chennai. She has published more than 15 papers in journals and conferences. She has also filed an Indian patent in the year 2021. She can be contacted at email: [kalpanag@srmist.edu.in](mailto:kalpanag@srmist.edu.in).